GEOPHYSICAL RESEARCH LETTERS, VOL. 34, L06103, DOI:10.1029/2008GL036805, 2009

Mirror instability: From quasi-linear diffusion to coherent structures

P. Hellinger,[1] E. A. Kuznetsov,[2] T. Passot,[3] P. L. Sulem[3] and P. M. Trávníček[1]

A model for the nonlinear dynamics of mirror modes near the instability threshold is presented. By matching the quasi-linear theory for the space-averaged distribution function with a reductive perturbative description of the mirror modes, the model reproduces the early-time flattening of the distribution function and the development of magnetic humps from an initial noise, in agreement with Vlasov-Maxwell numerical simulations. It suggests a possible mechanism at the origin of the mirror structures observed in planetary magnetosheaths and in the solar wind.

1. Introduction

Pressure-balanced magnetic structures in the form of magnetic enhancements (humps/peaks) and depressions (holes/dips) with a small change in the magnetic field direction that are observed in the solar wind [*Winterhalter et al.*, 1995] and in planetary magnetosheaths [*Joy et al.*, 2006] are often associated with the nonlinear evolution of the mirror instability [*Vedenov and Sagdeev*, 1958]. The understanding of the nonlinear processes involved in the saturation of this instability remains nevertheless incomplete. In spite of its aperiodic character, a quasi-linear (QL) theory was first developed by *Shapiro and Shevchenko* [1964] under the assumption that for each unstable wave vector $\boldsymbol{k}$, the growth rate $\gamma_{\boldsymbol{k}}$ is much smaller than $k_\parallel v_{\parallel th}$, where $v_{\parallel th}$ is the ion parallel thermal velocity and $k_\parallel$ is the parallel component of $\boldsymbol{k}$ (for the sake of simplicity, electrons are assumed to be cold). This approach which is usually assuming a random phase approximation and induces a diffusion in the velocity space, cannot describe regimes involving coherent structures. Phenomenological models, based on the cooling of trapped particles in magnetic troughs [*Kivelson and Southwood*, 1996; *Pantellini*, 1998], were constructed to explain the existence of deep magnetic holes, but hardly predict magnetic humps. In order to address the onset of coherent structures as the nonlinear development of the mirror instability, an asymptotic analysis near threshold, based on a reductive perturbative expansion of Vlasov-Maxwell (VM) equations was recently proposed [*Kuznetsov et al.*, 2007a; *Califano et al.*, 2008]. The resulting equation can be viewed as an extension of the dispersion relation of the mirror modes including the dominant nonlinear coupling whose effect is to reinforce the mirror instability, thus leading to a finite-time singularity associated with a subcritical bifurcation [*Kuznetsov et al.*, 2007b]. The form of this equation is generic, up to the coefficients which depend on the equilibrium distribution function. The sign of the nonlinear coupling coefficient prescribes in particular the geometry (magnetic holes or peaks) of the emerging structures. For a bi-Maxwellian distribution function, this coefficient is positive and the model predicts the formation of magnetic holes, while direct numerical simulations with the same initial conditions indicate the formation of magnetic humps. The formation of these structures is in fact preceded by a transient regime during which the distribution function displays a significant flattening, reminiscent of a quasi-linear evolution. The aim of the present paper is to suggest a possible matching of the two descriptions, aimed at qualitatively reproducing the numerical observations.

[1] Institute of Atmospheric Physics and Astronomical Institute, AS CR, Prague, Czech Republic

[2] Lebedev Physical Institute and Space Research Institute, Moscow, Russia

[3] Université de Nice-Sophia Antipolis, CNRS, Observatoire de la Côte d'Azur, Nice, France

0094-8276/09/2008GL036805$5.00

2. Quasi-linear description

2.1. The quasi-linear model

The QL approximation assumes a wide spectrum of non-coherent random-phase modes (or a sufficient overlapping of resonances). The modes are supposed to have low amplitudes together with slowly varying frequency (and growth/damping rate), so that they can be treated at the linear level. At the second order, they react on the distribution function, which leads to a slow diffusion for the velocity distribution function averaged over the space variables and the gyroangle:

$$\frac{\partial f}{\partial t} = \frac{\partial}{\partial v_\parallel} D_{\parallel\parallel} \frac{\partial f}{\partial v_\parallel} + \frac{1}{v_\perp}\frac{\partial}{\partial v_\perp} v_\perp \left(D_{\perp\parallel} \frac{\partial f}{\partial v_\parallel} + D_{\perp\perp} \frac{\partial f}{\partial v_\perp} \right) \tag{1}$$

with

$$\begin{aligned} D_{\parallel\parallel} &= v_\perp^4 \sum_{\boldsymbol{k}} \frac{|b_{\boldsymbol{k}}|^2}{4} \frac{\gamma_{\boldsymbol{k}} k_\parallel^2}{k_\parallel^2 v_\parallel^2 + \gamma_{\boldsymbol{k}}^2}, \quad D_{\perp\parallel} = -2\frac{v_\parallel}{v_\perp} D_{\parallel\parallel} \\ D_{\perp\perp} &= v_\perp^2 \sum_{\boldsymbol{k}} \gamma_{\boldsymbol{k}} \frac{|b_{\boldsymbol{k}}|^2}{4}, \end{aligned} \tag{2}$$

where the normalized magnetic fluctuations $b_{\boldsymbol{k}} = \delta B_z(\boldsymbol{k})/B_0$ obey $\frac{\partial b_{\boldsymbol{k}}}{\partial t} = \gamma_{\boldsymbol{k}} b_{\boldsymbol{k}}$s. The system is closed by using this instantaneous distribution function $f(v_\parallel^2, v_\perp, t)$, which gives the threshold condition $\Gamma = \beta_\Gamma - \beta_\perp - 1 > 0$ and the linear growth rate $\gamma_{\boldsymbol{k}} = \sqrt{\frac{2}{\pi}} |k_\parallel| \tilde{v} \Big(\Gamma - \frac{3}{2}\tilde{r}^2 k_\perp^2 - \frac{k_\parallel^2}{k_\perp^2}\chi \Big)$, where $k_\perp$ is the transverse component of $\boldsymbol{k}$ and

$$\beta_\perp = \frac{mn}{p_B} \int \frac{v_\perp^2}{2} f d^3v, \text{ and } \beta_\Gamma = -\frac{mn}{p_B} \int \frac{v_\perp^4}{4} \frac{\partial f}{\partial v_\parallel^2} d^3v. \tag{3}$$

Here n is the background density of the protons, m their mass, and $p_B = B_0^2/8\pi$ denotes the background magnetic pressure. Furthermore, near threshold, one has the positive coefficients [*Hellinger*, 2007] (Ω denoting the proton gyrofrequency),

$$\chi = 1 + \frac{1}{2}(\beta_\perp - \beta_\parallel) \text{ with } \beta_\parallel = \frac{mn}{p_B} \int v_\parallel^2 f d^3v, \tag{4}$$

$$\tilde{v}^{-1} = -\sqrt{2\pi} \frac{mn}{p_B} \int \frac{v_\perp^4}{4} \delta(v_\parallel) \frac{\partial f}{\partial v_\parallel^2} d^3v \tag{5}$$

$$\tilde{r}^2 = -\frac{mn}{24 p_B} \frac{1}{\Omega^2} \int \left(v_\perp^6 \frac{\partial f}{\partial v_\parallel^2} + 3 v_\perp^4 f \right) d^3v. \tag{6}$$

2.2. The numerical algorithm

We restrict ourselves to the case where the problem is one-dimensional in the space variable. The angle θ_{kB} between $\boldsymbol{k}$ and the ambient magnetic field is fixed to the value corresponding to the most unstable direction, leading to $k_\parallel = k\cos\theta_{kB}$, $k_\perp = k\sin\theta_{kB}$. The distribution function is conveniently written as a sum of the initial bi-Maxwellian contribution

$$f^{(0)} = \frac{1}{(2\pi)^{3/2} v_{th\parallel} v_{th\perp}^2} \exp\big(-\frac{v_\parallel^2}{2v_{th\parallel}^2} - \frac{v_\perp^2}{2v_{th\perp}^2}\big), \quad (7)$$

and the variation δf.

For the numerical simulation of the QL system, the distribution function δf is defined on a two-dimensional grid $\delta f_{i,j} = \delta f[(i-1/2)\Delta v_\parallel, (j-1/2)\Delta v_\perp]$ with $i = 0,\dots,N_\parallel+1$ and $j = 0,\dots,N_\perp+1$; only a quarter of the distribution function is considered, due to the assumed symmetries $\delta f(v_\parallel, v_\perp) = \delta f(\pm v_\parallel, \pm v_\perp)$. This is reflected in the inner boundary conditions $\delta f_{0,j} = \delta f_{1,j}$ and $\delta f_{i,0} = \delta f_{i,1}$. For the outer boundary conditions, we assume zero derivatives, $\delta f_{N_\parallel+1,j} = \delta f_{N_\parallel,j}$ and $\delta f_{i,N_\perp+1} = \delta f_{i,N_\perp}$. The wavenumber variable k is discretized as $k_m = m\Delta k$, $m = 1,\dots,N_k$.

For solving the diffusion equation (1), the partially implicit duFort-Frankel method is used, with space-centered derivatives in the velocity space. This is a three level method requiring δf at times $n\Delta t$ and $(n-1)\Delta t$ (where Δt is the time step). The first time step is done using a forward time centered scheme. The magnetic modes b_k are advanced in a similar manner.

The calculation of various coefficients is performed by adding the initial bi-Maxwellian values $\beta_\perp = mnv_{th\perp}^2/p_B$, $\beta_\parallel = mnv_{th\parallel}^2/p_B$, $\beta_\Gamma = \beta_\perp^2/\beta_\parallel$, $\tilde v = v_{th\parallel}/\beta_\Gamma$ and $\tilde r = v_{th\perp}(\beta_\Gamma - \beta_\perp)^{1/2}/\Omega$ to the contributions originating from δf. The integration over $v_\parallel$ and $v_\perp$ is replaced by the summation over i (from 1 to $N_\parallel$) and j (from 1 to $N_\perp$). To calculate $\tilde v$, we fit the quantity $\int_0^\infty v_\perp^4 \delta f dv_\perp$ around 0 by a polynomial $a_0 + a_1 v_\parallel^2 + a_2 v_\parallel^4$; the coefficient a_1 is then used to evaluate the contribution from δf to $\tilde v$.

In the following simulations, we use initial conditions such that $\beta_\parallel = 1$ and $\beta_\perp = 1.65$, which gives $\Gamma = 0.0725$, thus ensuring that the system is close to threshold. We choose $\theta_{kB} = 83.3^\circ$, because this angle corresponds to the maximum growth rate $\max(\gamma) = 1.03\cdot 10^{-4}\Omega$, reached for $k = 0.118\Omega/v_A$. The numerical parameters are $\Delta k = 9.2\cdot 10^{-4}\Omega/v_A$, $N_k = 256$, $\Delta v_\parallel = 4.9\cdot 10^{-4} v_A$, $N_\parallel = 1024$, $\Delta v_\perp = 4.9\cdot 10^{-3} v_A$, $N_\perp = 1024$, $\Delta t = 0.2/\Omega$.

2.3. Quasi-linear evolution

Figure 1 shows the evolution of different quantities from the QL simulation. From left to right, the fluctuating magnetic energy $W_B = \sum_k |b_k|^2$, the distance from threshold Γ and the maximum growth rate $\max(\gamma)$ are displayed as functions of time. Initially, the wave energy increases exponentially, then the QL diffusion reduces Γ and consequently $\max(\gamma)$, making the system to approach marginal stability. During this evolution, $\tilde v$ slightly increases (by about 0.1 %) whereas $\tilde r$ decreases (by about 2 %) and χ remains essentially constant (its relative decay is of order 10^{-8}).

The QL diffusion strongly affects the resonant region. Figure 2 displays the proton distribution function at the end of the simulation ($t = 1.4\cdot 10^5/\Omega$): top panel provides a grayscale plot of $v_\perp \delta f$ as a function of $v_\parallel$ and $v_\perp$. We note a strong similarity with Figure 4 of *Califano et al.* [2008] which displays the same quantity obtained by direct numerical integration of VM equations, supporting the relevance of a QL description of the early stage of nonlinear mirror mode evolution.

The shape of the level lines of the distribution function in Figure 2 is easily interpreted by noting that for $v_\perp$ of order unity and $v_\parallel$ small but out of the resonance, the parallel diffusion $D_{\parallel\parallel}$ term is dominant in Equation (1). A simple analysis shows that at a fixed time the solution of the diffusion equation only depends on the self-similar coordinate $v_\parallel/v_\perp$ whereas, in the region of small $v_\parallel$ the self-similar variable is $v_\parallel/v_\perp^2$.

Bottom panel of Figure 2 plots the profile of $\delta f/f^{(0)}$ as a function of $v_\parallel$ for $v_\perp = 2v_A$ in the conditions of the top panel. In order to interpret this graph, a simple model can be considered for the longitudinal diffusion. Concentrating on the most unstable mode, we neglect the wave-vector summation and define a rescaled time by $d\tau = |b_k|^2 dt$. Furthermore, since $v_\perp \sim O(1)$, $k_\parallel \sim \epsilon$ and $\gamma_k \sim \epsilon^2$ (here $\epsilon = \Gamma/\chi \ll 1$), we may restrict ourselves to the model equation

$$\frac{\partial f}{\partial \tau} = \frac{\partial}{\partial v}\left(\frac{\epsilon^2}{v^2+\epsilon^2}\frac{\partial f}{\partial v}\right) \quad (8)$$

supplemented by the initial condition $f^{(0)} = \exp(-v^2/v_{th}^2)$ (up to an irrelevant multiplicative constant). The variation of the distribution function $\delta f = f - f^{(0)}$ then obeys

$$\frac{\partial \delta f}{\partial \tau} - \frac{\partial}{\partial v}\frac{\epsilon^2}{v^2+\epsilon^2}\frac{\partial \delta f}{\partial v} = \frac{\partial}{\partial v}\left(\frac{\epsilon^2}{v^2+\epsilon^2}\frac{\partial f^{(0)}}{\partial v}\right). \quad (9)$$

Assuming $v \ll v_{th}$, we have for the source term S, defined as the r.h.s. of Equation (9),

$$S \approx \frac{2}{v_{th}^2}\,\frac{\epsilon^2}{v^2+\epsilon^2}\,\frac{v^2-\epsilon^2}{v^2+\epsilon^2}. \quad (10)$$

S has a minimum at 0, $S(0) = -2/v_{th}^2$ and two maxima for $v = \pm\sqrt{3}\epsilon$, equal to $1/4v_{th}^2$. Its profile is qualitatively similar to that of δf in Figure 2 (bottom panel). Thus S is of order unity in the small-velocity range we are interested in, while its typical scale (in the v variable) is of order ϵ. As a consequence δf will also have the same typical scale in v. Furthermore, after a typical diffusion time $\tau \sim \epsilon^2$, we have $\delta f \sim \epsilon^2$. Coming back to the physical time, we write $t = \tau/|b_k|^2 \sim \epsilon^2/|b_k|^2$. Estimating the level of saturation of the magnetic fluctuations by balancing the diffusion time $\epsilon^2/\sum_{\boldsymbol{k}} |b_k|^2$ and the inverse growth time $1/\epsilon^2$, gives at the saturation time $\sum_{\boldsymbol{k}} |b_k|^2 \sim \epsilon^4$, in agreement with the numerics where $\epsilon = 10^{-2}$ (as estimated from $\gamma_k = 10^{-4}$) and where $\sum_{\boldsymbol{k}} |b_k|^2 \sim 10^{-8}$ at the saturation time $t \sim 5\cdot 10^4$.

3. Onset of coherent structures

To address the regime of structure formation, the reductive perturbative expansion near threshold developed in *Kuznetsov et al.* [2007a]; *Califano et al.* [2008], may be easily extended to any (frozen) smooth equilibrium distribution function $f(v_\parallel^2, v_\perp)$ (provided $\tilde v > 0$, $\tilde r^2 > 0$, and $\chi > 0$). It leads to an equation for the (normalized) parallel perturbation of the magnetic field, $b = \delta B_z(\boldsymbol{r}, t)/B_0$, of the form

$$\partial_t b = \sqrt{\frac{2}{\pi}}\tilde v\,(-\mathcal{H}\partial_z)\left(\Gamma b + \frac{3}{2}\tilde r^2 \Delta_\perp b - \chi\frac{\partial_z^2}{\Delta_\perp} b - \Lambda b^2\right). \quad (11)$$

The linear part of this equation reproduces the linear growth rate, whereas the nonlinear term involves a coefficient Λ given by

$$\Lambda = \beta_\Lambda - 2\beta_\Gamma + \frac{\beta_\perp}{2} + \frac{1}{2} \text{ with } \beta_\Lambda = \frac{mn}{p_B}\int \frac{v_\perp^6}{8}\frac{\partial^2 f}{\partial (v_\parallel^2)^2} d^3v, \quad (12)$$

where for a bi-Maxwellian distribution we have $\beta_\Lambda = 3/2\beta_\perp^3/\beta_\parallel^2$. These results are obtained by neglecting the contribution of resonant particles whose effect is subdominant in the case of a smooth distribution function with no sharp variations. Similar results were obtained using the drift-kinetic approach by *Pokhotelov et al.*

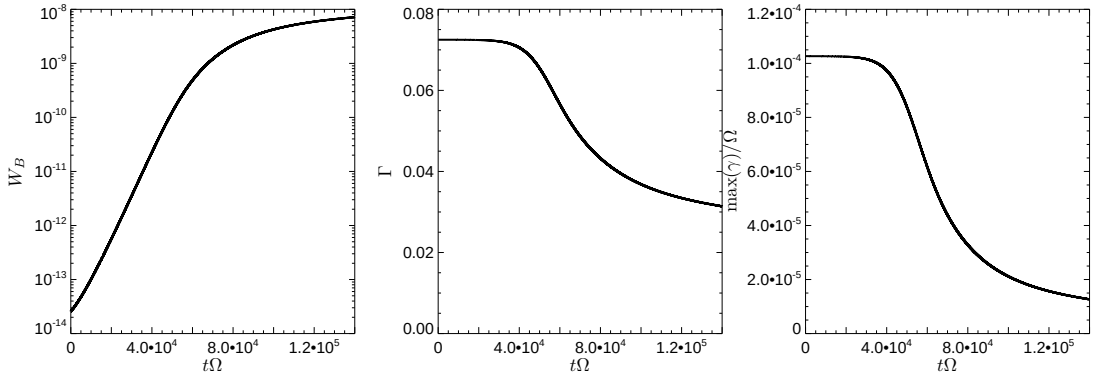

Figure 1. Results of the QL simulation: (top) fluctuating magnetic energy $W_B = \sum_k |b_k|^2$, (middle) distance from threshold Γ, (bottom) maximum growth rate $\max(\gamma)$ as functions of time.

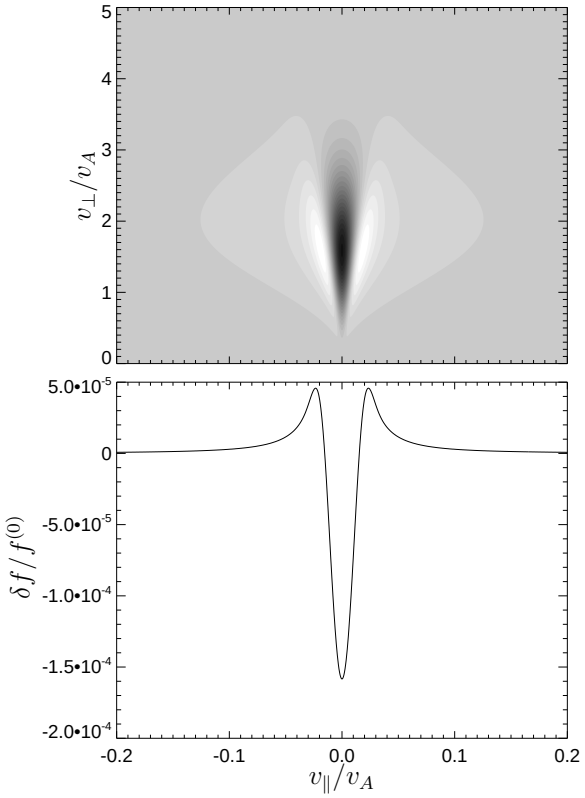

Figure 2. Results of the QL simulation at $t = 1.4 \cdot 10^5/\Omega$: (top) Gray scale plot of $v_\perp \delta f$ as a function of $v_\parallel$ and $v_\perp$. Black corresponds to negative values and white to positive ones; (bottom) Profile of $\delta f/f^{(0)}$ as a function of $v_\parallel$ at $v_\perp = 2v_A$.

[2008]. We note here that most of the criticism of this paper with respect to *Kuznetsov et al.* [2007a] is due to a misunderstanding about the used variables.

In order to take into account the QL regime observed at early time in VM simulations, we are led to modify the non-linear asymptotic equation (11), by assuming that the coefficients are not frozen to their initial values but are evaluated from the instantaneous distribution function given by the QL diffusion equation. The computation of the coefficient Λ needs however to be revisited because, as previously mentioned, the QL evolution predicts that in the time of order $1/\epsilon^2$ needed for the nonlinearity to become relevant, the perturbation of the distribution function satisfies $\delta f \sim \epsilon^2$. Since the typical variation takes place on a parallel velocity range of order ϵ, it follows that $\partial^2 f/(\partial v_\parallel^2)^2 \sim 1/\epsilon^2$ near $v_\parallel = 0$, leading to $\beta_\Lambda \sim 1/\epsilon$ because the effective integration range on the $v_\parallel$ is of order ϵ. The contribution of the resonant particles can thus no longer be neglected in the evaluation of the nonlinear coupling. The magnitude of all the other coefficients remain in contrast correctly estimated.

In order to retain the contribution of the resonant particles to β_Λ, we return to the pressure balance equation as given in *Califano et al.* [2008], and retain the full contribution to β_Λ that is no longer a number but becomes the operator

$$\mathcal{B} = \frac{mn}{p_B} \int \frac{v_\perp^6}{8} \frac{v_\parallel \partial_z}{\partial_t + v_\parallel \partial_z} \frac{\partial^2 f}{(\partial v_\parallel^2)^2} d^3v. \qquad (13)$$

Neglecting the time derivative indeed reproduces β_Λ. From the Plemenj formula, it follows that

$$\mathcal{B} = \beta_\Lambda + \sqrt{\frac{\pi}{2}} v_\Lambda^{-1} (-\mathcal{H}\partial_z)^{-1} \partial_t \tag{14}$$

with

$$v_\Lambda^{-1} = \sqrt{2\pi} \frac{mn}{p_B} \int \frac{v_\perp^6}{8} \delta(v_\parallel) \frac{\partial^2 f}{(\partial v_\parallel^2)^2} d^3v, \tag{15}$$

whose initial bi-Maxwellian value is $v_{th\parallel}/\beta_\Lambda$. This finally leads to

$$\partial_t b = \frac{\sqrt{\frac{2}{\pi}}\tilde{v}}{1 + 2\frac{\tilde{v}}{v_\Lambda} b} (-\mathcal{H}\partial_z) \left(\Gamma b + \frac{3}{2}\tilde{r}^2 \Delta_\perp b - \chi \frac{\partial_z^2}{\Delta_\perp} b - \Lambda b^2 \right). \tag{16}$$

The presence of a denominator in the right-hand side of equation (16) reminds one of the phenomenological correction to equation (11) suggested by *Pokhotelov et al.* [2008] to model the flattening of the distribution function. A main difference originates from the dynamical evolution of the coefficients involved in our description.

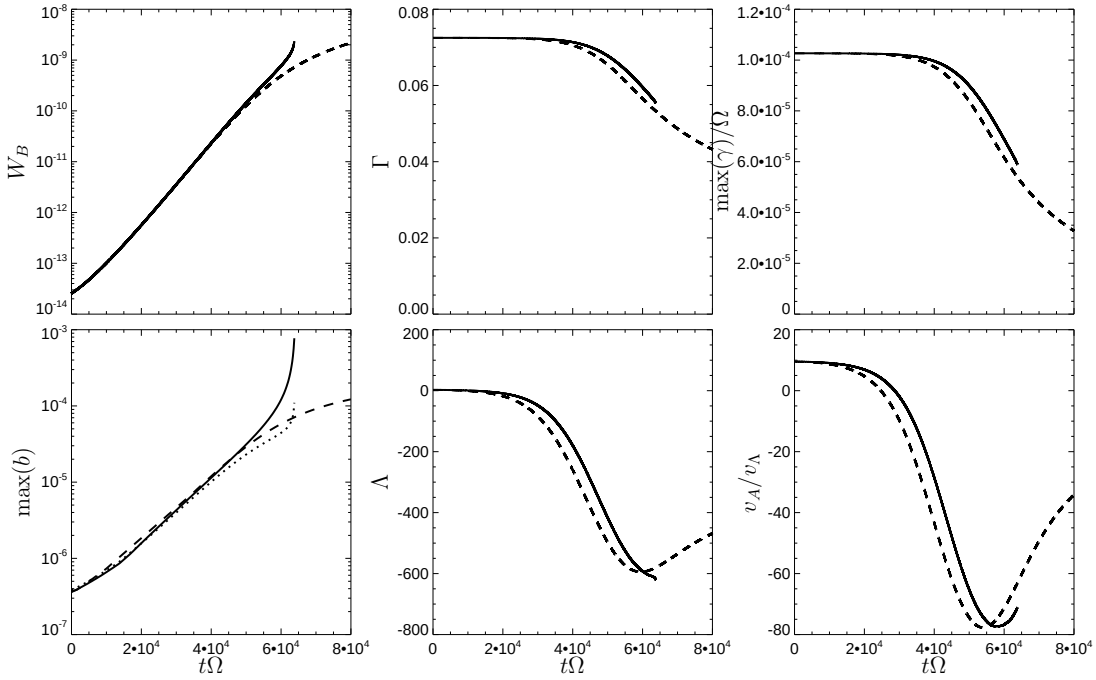

Figure 3. Results of the simulation of equation (16): solid lines show the time evolution of(from left to right, from top to bottom) $W_B = \sum_k |b_k|^2$, Γ, maximum of γ_k, maximum of the magnetic fluctuations $b(x)$, Λ and v_Λ^{-1}. For comparison, dashed lines show the evolution in the QL model. The dotted line in the left-bottom panel refers to the evolution of the maximum of $-b(x)$, as predicted by equation (16).

Let us investigate the predictions of our model that retains the diffusion equation of the QL theory for the distribution function, but prescribes the nonlinear equation (16) for the evolution of the magnetic fluctuations. Figure 3 shows the time variation of different quantities as obtained by the numerical integration of this model (solid line), using the same initial conditions as for the QL simulation. From left to right and top to bottom, it displays the time evolution of the energy of the parallel magnetic fluctuations W_B, the distance to threshold Γ, the growth rate γ_k of the most unstable mode, the maximum of the magnetic fluctuations $b(x)$, together with the coefficients Λ and v_Λ^{-1}, as functions of time. The dotted line in the left-bottom panel corresponds to the time variation of the maximum of $-b(x)$. For comparison, the dashed curves show the evolution in the QL model (see Figure 1).

We observe that for a while, the dynamics is essentially described by the QL model, but a departure is observed when the QL evolution tends to saturate the magnetic field fluctuations. In this model, the magnetic energy continues to grow and the maximum of b(x) displays a sharp increase suggesting a finite-time blowup, consistent with a subcritical bifurcation [*Kuznetsov et al.*, 2007b]. The computation should thus be interrupted due to the lack of resolution. The arrest of

the singularity would require additional effects, not retained in the present model, such as nonlinear finite Larmor radius corrections [*Kuznetsov et al.*, 2007a]. Figure 4 shows the profile of the magnetic fluctuations b at $t = 6.3 \cdot 10^4$, shortly before the numerical explosion. We observe that the present model predicts the formation of magnetic humps, in agreement with the VM numerical simulations. The reason is that the early QL evolution leads to a change of sign of Λ which, being initially positive, becomes strongly negative. A similar evolution is observed in VM direct simulation [*Califano et al.*, 2008, section 4.1] (which starts further from threshold, $\Gamma = 0.6$) where Λ evolves from 6 to about -30. In the context of the QL evolution that predicts a $1/\epsilon$ scaling for Λ it is not surprising that the model gives an even larger magnitude of Λ. Nevertheless, further corrective terms with regularizing effects could possibly act near threshold, beyond the denominator in the right-hand side of equation (16) which also involve a relatively large coefficient. Particle trapping could for example partially inhibit QL effects [*Pantellini et al.*, 1995], without changing the global features of the dynamics.

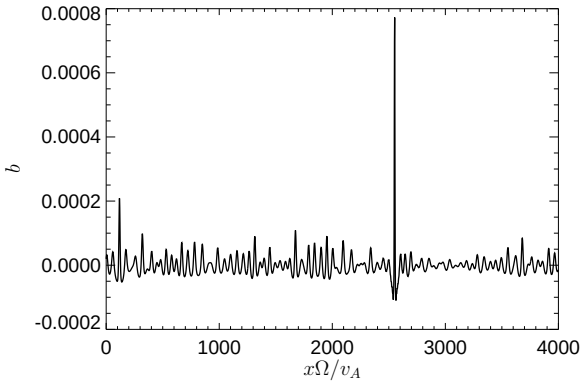

Figure 4. Results of the simulation of equation (16): b as a function of x at $t = 6.3 \cdot 10^4$

4. Conclusion

Quasi-linear evolution of the mirror instability was investigated by direct integration of the corresponding diffusion equation. The resulting flattening of the distribution function is in good agreement with the early time results of Vlasov-Maxwell simulations. A dynamical model was then presented that reproduces the formation of mirror structures observed at later times. It provides a possible mechanism for the formation of magnetic humps in a mirror unstable plasma, as revealed by satellite measurements. A main characteristic of the present model is the role of kinetic effects that lead to small-amplitude but very sharp variations of the parallel-velocity distribution function of the resonant particles, which eventually prescribes the geometry of the emerging structures.

Acknowledgments. This work was performed in the framework of the Barrande-Egide project 14226SH. The work of TP and PLS was supported by Programme Terre Soleil of CNRS. EK acknowledges support of RFBR grant no. 06-01-00665, and PH and PMT of GAAV grant No. IAA300420702 and IAA300420602. Visits of EK and PH at OCA were supported by the French Ministère de l'Enseignement Supérieur et de la Recherche.

References

Califano, C., P. Hellinger, E. Kuznetsov, T. Passot, P.-L. Sulem, and P. M. Trávníček (2008), Nonlinear mirror mode dynamics: Simulations and modeling, *J. Geophys. Res.*, *113*, A08219, doi:10.1029/2007JA012898.

Hellinger, P. (2007), Comment on the linear mirror instability near the threshold, *Phys. Plasmas*, *14*, 082105.

Joy, S. P., M. G. Kivelson, R. J. Walker, K. K. Khurana, C. T. Russell, and W. R. Paterson (2006), Mirror mode structures in the Jovian magnetosheath, *J. Geophys. Res.*, *111*, A12212, doi:10.1029/2006JA011985.

Kivelson, M. G., and D. J. Southwood (1996), Mirror instability II: The mechanism of nonlinear saturation, *J. Geophys. Res.*, *101*, 17,365–17,372.

Kuznetsov, E. A., T. Passot, and P.-L. Sulem (2007a), Dynamical model for nonlinear mirror modes near threshold, *Phys. Rev. Lett.*, *98*, 235,003.

Kuznetsov, E. A., T. Passot, and P.-L. Sulem (2007b), Nonlinear theory of mirror instability near threshold, *JETP Lett.*, *86*, 637–642.

Pantellini, F. G. E. (1998), A model of the formation of stable nonpropagating magnetic structures in the solar wind based on the mirror instability, *J. Geophys. Res.*, *103*, 4789–4798.

Pantellini, F. G. E., D. Burgers, and S. J. Schwartz (1995), On the non-linear mirror instability, *Adv. Space Res.*, *15*, 341–344.

Pokhotelov, O. A., R. Z. Sagdeev, M. A. Balikhin, O. G. Onishchenko, and V. N. Fedun (2008), Nonlinear mirror waves in non-Maxwellian space plasmas, *J. Geophys. Res.*, *113*, A04225, doi:10.1029/2007JA012642.

Shapiro, V. D., and V. I. Shevchenko (1964), Quasilinear theory of instability of a plasma with an anisotropic ion velocity distribution, *Sov. Phys. JETP, Engl. Transl.*, *18*, 1109–1116.

Vedenov, A. A., and R. Z. Sagdeev (1958), Some properties of a plasma with an anisotropic ion velocity distribution in a magnetic field, in *Plasma Physics and the Problem of Controlled Thermonuclear Reactions*, vol. 3, pp. 332–339, Pergamon, New York.

Winterhalter, D., M. Neugebauer, B. E. Goldstein, E. J. Smith, B. T. Tsurutani, S. J. Bame, and A. Balogh (1995), Magnetic holes in the solar wind and their relation to mirror-mode structures, *Space Sci. Rev.*, *72*, 201–204.

P. Hellinger and P. M. Trávníček Institute of Atmospheric Physics and Astronomical Institute, AS CR, Prague 14131, Czech Republic. (petr.hellinger@ufa.cas.cz, trav@ig.cas.cz)

E. A. Kuznetsov, P.N. Lebedev Physical Institute, 53 Leninsky Avenue, 119991 Moscow, Russia and Space Research Institute, 84/31 Profsoyuznaya Street, 117997 Moscow, Russia (kuznetso@itp.ac.ru)

T. Passot and P.L. Sulem, Université de Nice-Sophia Antipolis, CNRS, Observatoire de la Côte d'Azur, B.P. 4229, 06304 Nice Cedex 4, France (passot@oca.eu, sulem@oca.eu)